INVITED PAPER

Sparsity and Compressed Sensing in Radar Imaging

The success and accuracy of remote sensing with Radar can be predicted from reasonably limited samples of Radar signals.

By Lee C. Potter, *Senior Member IEEE*, Emre Ertin, *Member IEEE*, Jason T. Parker, *Member IEEE*, and Müjdat Çetin, *Member IEEE*

ABSTRACT | Remote sensing with radar is typically an ill-posed linear inverse problem: a scene is to be inferred from limited measurements of scattered electric fields. Parsimonious models provide a compressed representation of the unknown scene and offer a means for regularizing the inversion task. The emerging field of compressed sensing combines nonlinear reconstruction algorithms and pseudorandom linear measurements to provide reconstruction guarantees for sparse solutions to linear inverse problems. This paper surveys the use of sparse reconstruction algorithms and randomized measurement strategies in radar processing. Although the two themes have a long history in radar literature, the accessible framework provided by compressed sensing illuminates the impact of joining these themes. Potential future directions are conjectured both for extension of theory motivated by practice and for modification of practice based on theoretical insights.

KEYWORDS | Moving target indication; penalized least squares; radar ambiguity function; random arrays; sparse reconstruction; synthetic aperture radar

Manuscript received April 21, 2009; revised September 2, 2009; accepted November 5, 2009. Date of publication February 25, 2010; date of current version May 19, 2010. This work was supported in part by AFOSR under Award FA9550-06-1-0324. The work of J. T. Parker was supported by AFOSR.

L. C. Potter and **E. Ertin** are with the Department of Electrical and Computer Engineering, The Ohio State University, Columbus, OH 43210 USA (e-mail: potter.36@osu.edu; ertine@ece.osu.edu).
J. T. Parker is with the Air Force Research Laboratory Sensors Directorate, Wright Patterson AFB, OH 45433-5543 USA (e-mail: jason.parker@wpafb.af.mil).
M. Çetin is with Sabancı University, Istanbul 34956, Turkey (e-mail: mcetin@sabanciuniv.edu).

Digital Object Identifier: 10.1109/JPROC.2009.2037526

I. INTRODUCTION

Radar imaging is an inverse scattering problem whereby a spatial map of reflectivity is reconstructed from measurements of scattered electric fields. Imaging techniques to exploit parsimony in sparse or compressible scenes have been proposed throughout the 60-year development of radar processing for suppression of sidelobes and super-resolution of scattering locations. Many radar processing tasks can be posed as finding sparse solutions to underdetermined linear equations—a topic addressed by the emerging field of compressed sensing (CS).

The primary interest in compressed sensing research is the inverse problem of recovering a signal $\boldsymbol{f} \in \mathbb{C}^N$ from noisy linear measurements $y = \boldsymbol{A}\boldsymbol{f} + \boldsymbol{n} \in \mathbb{C}^M$ [1], [2]. The focus is on underdetermined problems where the forward operator $\boldsymbol{A} \in \mathbb{C}^{M\times N}$ has unit norm columns and forms an incomplete basis with $M \ll N$. The resulting ill-posed inverse problem is regularized assuming 1) that the unknown signal $\boldsymbol{f}$ is K-sparse (i.e., has at most K nonzero entries) or is compressible with K significant coefficients and 2) the noise process is bounded by $\|\boldsymbol{n}\|_2 < \epsilon$. CS theory provides strong results which guarantee stable solution of the sparse signal recovery problem for a class of forward operators $\boldsymbol{A}$ that satisfies certain properties. One such class of operators is defined by bounding the singular values of the submatrices of $\boldsymbol{A}$. Specifically, the *restricted isometry constant* (RIC) δ_K for forward operator $\boldsymbol{A}$ is the smallest $\delta \in (0,1)$ such that

$$(1-\delta_K)\|\boldsymbol{x}\|_2^2 \le \|\boldsymbol{A}\boldsymbol{x}\|_2^2 \le (1+\delta_K)\|\boldsymbol{x}\|_2^2 \qquad (1)$$

holds for all vectors $\boldsymbol{x}$ with at most K nonzero entries.

One of the key contributions of CS is that stable recovery of compressible, noisy signals can be achieved through the solution of the computationally tractable ℓ_1 regularized inverse problem

$$\min_{f} \|\boldsymbol{f}\|_1 \text{ subject to } \|\boldsymbol{A}\boldsymbol{f}-\boldsymbol{y}\|_2^2 \leq \epsilon^2. \tag{2}$$

At present, the least conservative available bound on the reconstruction performance [3] guarantees that if $\delta_{2K} < \sqrt{2}-1$ and $\|\boldsymbol{n}\|_2 \leq \epsilon$, then the solution $\hat{\boldsymbol{f}}$ to (2) will satisfy

$$\|\boldsymbol{f}^* - \hat{\boldsymbol{f}}\|_2 \leq C_0 K^{\frac{-1}{2}} \|\boldsymbol{f}^* - \boldsymbol{f}_K\|_1 + C_1\epsilon \tag{3}$$

where $\boldsymbol{f}_K$ is the best K-sparse approximation to the true solution $\boldsymbol{f}^*$, C_0 and C_1 are small constants, and $\|\cdot\|_p$ represents the ℓ_p norm. The optimization in (2) can be viewed as the convex relaxation [4] of the NP-hard task of finding the sparsest feasible solution

$$\min_{f} \|\boldsymbol{f}\|_0 \text{ subject to } \|\boldsymbol{A}\boldsymbol{f}-\boldsymbol{y}\|_2^2 \leq \epsilon \tag{4}$$

where $\|\cdot\|_0$ is the ℓ_0 norm, i.e., the number of nonzero entries in the vector. In radar and other array processing applications, imperfect calibration implies that precise knowledge of $\boldsymbol{A}$ is not available. Recent work [5] has shown that a bounded unknown additive disturbance to the matrix $\boldsymbol{A}$ still permits a RIC-based guarantee on reconstruction performance that reduces to the result in [3] as the disturbance bound approaches zero.

For large M, estimating and testing the RIC is impractical. A tractable yet conservative bound on the RIC can be obtained through the *mutual coherence* of the columns of $\boldsymbol{A}$ defined as

$$\mu(\boldsymbol{A}) = \max_{i\neq j} \left|\boldsymbol{a}_i^H \boldsymbol{a}_j\right|. \tag{5}$$

Mutual coherence can be used to guarantee stable inversion through ℓ_1 recovery (2) [6]. Furthermore, the RIC is conservatively bounded by $\delta_K \leq (K-1)\mu(\vec{A})$.

We note that this mutual coherence notion is quite different from the coherency concept in radar systems. Typical radar systems process returns from multiple pulses to estimate location and velocity information of the targets in the scene. Coherent radar systems maintain a high level of phase coherency from pulse to pulse, enabling joint processing of the phase information from a collection of pulses spanning the coherent processing interval (CPI). In contrast, noncoherent radar systems encounter a random phase error from pulse to pulse, limiting the receive processing to the magnitude of the returns. To minimize the confusion between the two notions of coherency in CS and radar, we use the term *phase coherency* for the latter.

Compressed sensing combines three elements: linear models with low coherence among regressors, low-complexity nonlinear reconstruction algorithms, and, most significantly, sufficient conditions for provably stable reconstruction. The performance guarantees have validated the long-standing use of various sparse reconstruction algorithms, have spurred resurgent use of pseduorandom waveforms or radar apertures for low coherence, and have illuminated the utility in combining these two separate practices.

In this paper, we survey the roles of sparsity and CS elements in existing radar imaging practice, linking coherence and algorithms to analogous concepts in radar. Further, we offer opinions on the potential impact of CS insights on future directions of radar imaging. In Section II, we sketch radar imaging as a linear inverse problem. Section III gives an overview of the use of sparse reconstruction algorithms, coherence, and spectrum estimation in radar imaging. Example applications of sparsity and CS concepts in radar are presented as vignettes in Section IV. Section V concludes with a discussion of conjectured directions of future inquiry.

II. RADAR IMAGING

Radar signal processing encompasses a wide diversity of applications, sensing objectives, processing techniques, propagation media, and sensor configurations, e.g., [7]–[11]. This section seeks merely to provide an introduction to some of the key ideas in radar imaging to facilitate the reader's appreciation of the CS radar vignettes provided in Section IV. For simplicity, this paper will model reflected radar signals using free space propagation, narrow bandwidths, relatively slow targets, far-field plane waves, and a linear, i.e., single bounce (Born) scattering approximation. This treatment is standard and follows naturally from a careful analysis of the scalar wave equation; see, e.g., [12]. The resulting linear model can be adapted quite easily to the CS framework, as shown below.

A. Monostatic Radar

We first consider the case of a radar with narrow fractional bandwidth and monostatic operation, i.e., colocated transmitter and receiver antennas. A complex baseband pulse $u(t)$ is modulated in quadrature by a carrier with frequency ω_c to yield the transmit waveform $p(t) = \mathrm{Re}\{u(t)e^{j\omega_c t}\}$, where $\mathrm{Re}\{\}$ denotes the real operator. The echo of the transmitted pulse waveform encodes backscatter energy from the illuminated scene. Assume the illuminated scene consists of scatterers at range r with radial velocity v. We can parameterize the complex scene reflectivity in terms of delay and Doppler as $f(\tau,\omega)$, where $\tau(r) = 2r/c$ is the round-trip propagation time and

$\omega(v) = 2w_c v/c$ is the Doppler shift. The total received signal backscattered from the scene is then given by

$$y(t) = \mathrm{Re}\left\{ \iint f(\tau(r), \omega(v)) u(t - \tau(r)) \times e^{j(w_c - \omega(v))(t-\tau(r))}\, dr\, dv \right\} + n(t) \quad (6)$$

where $n(t)$ is assumed to be white Gaussian noise arising from thermal noise in the transmitter and receiver hardware. Upon receive, quadrature demodulation yields the complex baseband signal

$$y_B(t) = \iint f(\tau, \omega) u(t-\tau) e^{-j\omega t}\, d\tau\, d\omega + n_B(t) \quad (7)$$

where the constant phase terms have been absorbed into the reflectivity and $n_B(t)$ represents the circular white complex Gaussian baseband noise. The basic radar problem is to estimate the reflectivity $f(\tau, \omega)$ of the scatterers in the scene. The likelihood ratio test statistic for the existence of a single target with delay τ' and Doppler frequency ω' is the matched filter output

$$\begin{aligned} \chi(\tau', \omega') &= \int y_B(t) u^*(t - \tau') e^{j\omega' t}\, dt \\ &= \iint f(\tau, \omega) \mathcal{A}(\tau - \tau', \omega - \omega')\, d\tau\, d\omega \\ &\quad + \int n_B(t) u^*(t-\tau') e^{j\omega' t}\, dt \end{aligned} \quad (8)$$

where the radar ambiguity function $\mathcal{A}(\tau, \omega)$ is given by $\mathcal{A}(\tau, \omega) = \int u(t) u^*(t-\tau) e^{j\omega t} dt$. Thus, the output of the matched filter is the convolution of the reflectivity $f(\tau, \omega)$ with the radar ambiguity function $\mathcal{A}(\tau, \omega)$, plus a filtered copy of the baseband noise. The shape of the ambiguity function can be adjusted by varying the pulse waveform $u(t)$. However, shaping of the ambiguity function is subject to a total volume constraint

$$\iint |\mathcal{A}(\tau, \omega)|^2\, d\tau\, d\omega = \|u(t)\|_2^2. \quad (9)$$

Therefore, the matched filter response cannot resolve scatterers perfectly in delay and Doppler simultaneously, and an ambiguity function with a sharper central peak will necessarily have higher sidelobes to satisfy this constraint.

This model can be easily adapted for use with the CS framework. If we discretize the scene reflectivity function f over range and Doppler on a grid of points $\{\tau_m, \omega_m\}$ to produce the vector $\boldsymbol{f}$ and sample the received baseband signal y_B at times $\{t_m\}$ to obtain $\boldsymbol{y}$, we obtain the linear system of equations

$$\boldsymbol{y} = \boldsymbol{A}\boldsymbol{f} + \boldsymbol{n}. \quad (10)$$

Likewise, the sampled matched filter outputs can be written as

$$\chi = \boldsymbol{A}^H \boldsymbol{y}. \quad (11)$$

Each column $\boldsymbol{a}_i$ of $\boldsymbol{A}$ thus represents the received waveform for a scatterer with given Doppler and range, and all columns share the same 2-norm, under the far-field assumption. The coherence between the columns of the forward operator $\boldsymbol{A}$ is prescribed by the ambiguity function $|\boldsymbol{a}_i^H \boldsymbol{a}_j| = |\mathcal{A}(\tau_i - \tau_j, \omega_i - \omega_j)|$. The columns of $\boldsymbol{A}$ comprise a dictionary for representing $\boldsymbol{y}$, and the total volume constraint given in (9) constrains the mutual coherence of this dictionary.

B. Tomographic Perspective for Imaging

Imaging radars use antenna platform motion to interrogate a scene with pulses from a diverse set of angles to reveal the spatial distribution of the scatterers. If phase coherency is maintained at the receiver from pulse to pulse, then this motion effectively creates a larger aperture for processing, hence the common term synthetic aperture radar (SAR). We consider a stationary scene with spatial reflectivity function $f(\boldsymbol{r})$ parameterized by the spatial location $\boldsymbol{r}$, whose origin is fixed at scene center, and interrogated with pulses transmitted and received at locations $\{\boldsymbol{p}_m\}$. Note that the Doppler is assumed to be zero for all targets, and the variable $\boldsymbol{r}$ maps into a delay τ that depends on the position of the transmitter at each pulse.

For sufficiently short pulse durations, the platform motion during a pulse is negligible, owing to the high speed of electromagnetic propagation. As a result, radar signals are typically processed under the so called "stop-and-hop" approximation [8], in which the platform and all targets are assumed to be stationary during the transmission and reception of a given pulse. Reflector position is encoded in the phase shifts between successive received pulses; hence the importance of phase coherency in modern radars. In this light, the data collected by a SAR are conceptually the same as data collected in tomography applications, an algorithmically fruitful connection that was popularized in the radar community by [13].

High range resolution is achieved by high-bandwidth pulses with good autocorrelation properties. The linear FM chirp $p(t) = \mathrm{Re}\{w(t) e^{j(w_c t + \alpha t^2)}\}$, where $w(t)$ is a rectangular time window with pulse length of τ_c, is by far the most common choice, owing to simplicity in implementation and a constant modulus well suited to power amplifiers. The received echo from pulse m is given by

$$y(t,m) = \mathrm{Re}\left\{\int f(\boldsymbol{r})p\big(t-2\|\boldsymbol{r}-\boldsymbol{p}_m\|/c\big)\,d\boldsymbol{r}\right\}+n(t). \quad (12)$$

Upon receive, the chirp signal is typically deconvolved from the received echo signal using a deramp (or "dechirp") process by mixing the signal with the transmitted chirp and sampling at a rate determined by the scene size rather than the pulse bandwidth [10]. It can be shown that the output of the deramp processing represents samples of the Fourier transform of the Radon projection $\mathcal{P}_{\boldsymbol{p}_m}$ of the scene reflectivity orthogonal to the vector $\boldsymbol{p}_m$ for $\|\boldsymbol{p}_m-\boldsymbol{r}\| \gg \|\boldsymbol{r}\|$, i.e., under a far-field assumption. Because $P(\omega)P^*(\omega)$ is nearly constant across the passband $\mathcal{B}=(\omega_c-\alpha\tau_c, \omega+\alpha\tau_c)$, the samples are equalized across frequency

$$y_D(\omega,m) \approx \mathcal{F}\left[\mathcal{P}_{\boldsymbol{p}_m} f(\boldsymbol{r})\right], \quad \omega \in \mathcal{B}. \quad (13)$$

Finally, the projection-slice theorem relates the received signal to the samples of the spatial Fourier transform $F(\boldsymbol{k})$, where $\boldsymbol{k}$ is the spatial frequency of the reflectivity function $f(\boldsymbol{r})$

$$y_D(\omega,m) = F\left(\frac{2\omega}{c}\frac{\boldsymbol{p}_m}{\|\boldsymbol{p}_m\|}\right), \quad \omega \in \mathcal{B}. \quad (14)$$

Under the far-field assumption, this model for the received data can be easily extended to the bistatic case, i.e., where the transmitter and receiver are not colocated. In this case, for simplicity, we redefine $\boldsymbol{p}_m$ to be the bistatic bisector between the transmitter and receiver. Let θ_m be the bistatic angle between the two platforms for pulse m. Then, the collected data can be related to the Fourier transform of the reflectivity by [14], [15]

$$y_D(\omega,m) = F\left(\frac{2\omega}{c}\cos\left(\frac{\theta_m}{2}\right)\frac{\boldsymbol{p}_m}{\|\boldsymbol{p}_m\|}\right), \quad \omega \in \mathcal{B}. \quad (15)$$

Discretizing the frequency ω, the scene reflectivity $\boldsymbol{f}$, the dechirped received signal $\boldsymbol{y}$, and the noise $\boldsymbol{n}$, we obtain the linear system of equations

$$\boldsymbol{y} = \boldsymbol{A}\boldsymbol{f} + \boldsymbol{n} \quad (16)$$

where $\boldsymbol{y}$ represents a concatenation of the dechirped data from each pulse in the CPI, and $\boldsymbol{f}$ is a properly ordered vector of the reflectivities for the entire scene. The vector $\boldsymbol{n}$ represents a discretization of the baseband noise. Each column of the matrix $\boldsymbol{A}$ represents the set of dechirped samples across the complete CPI for a given point in the discretized scene.

This model can easily account for arbitrary waveforms, windowing, or alternative linear receiver processing; likewise, the index m may be generalized to include data from multiple transmitters and receivers. A more general development of the forward operator is provided in [16]. The development in this section has sought to emphasize that the forward operator $\boldsymbol{A}$ for imaging radars depends on both the transmit waveforms and the collection geometry given by the platform position vectors $\boldsymbol{p}_m$.

III. SPARSITY AND CS THEMES IN RADAR

The concepts of sparse reconstruction algorithms and mutual coherence are central themes in CS and have been present in five decades of array processing literature. This section presents a brief survey of these themes and their use in radar imaging while also drawing connections between the radar and CS literatures. Compressed sensing gives an easily accessible framework that illuminates the power of combining pseudorandomization (for low-coherence forward models $\boldsymbol{A}$) with sparse reconstruction algorithms.

A. Sparse Scenes

For high-resolution images at high frequencies, the scattering response of an object can be well approximated as a sum of responses from individual reflectors [17]. These scattering centers provide a concise, yet physically relevant, description of the object. For example, an approximate physical optics model for a set of canonical reflectors [18], [19] parameterizes responses as a function of frequency, incident angle, receive angle, and polarization. Fitting the models to measured data is a nonlinear regression task, with the accompanying challenges of computational cost, model selection, and local minima in the nonconvex optimization. For example, Fig. 1(a) and (b) shows images of a vehicle observed by a 9.6 GHz airborne radar at 45° elevation and full 360° azimuth orbits [20]. A single polarization image from eight orbits is given in Fig. 1(a), which displays the backprojection image $\boldsymbol{A}^H\boldsymbol{y}$ formed by matched filtering to a point reflector at each voxel location in a 1000 m^3 cube. The eight passes provide only a sparse sampling across less than 2° elevation and hence result in high sidelobes and aliasing in the backprojection image. Fig. 1(b) displays a sparse image formed by jointly processing copolarized images using nonlinear least squares estimation [21]. Scattering is parametrically modeled as the superposition of responses from plates and dihedrals [19]. Icons depict the

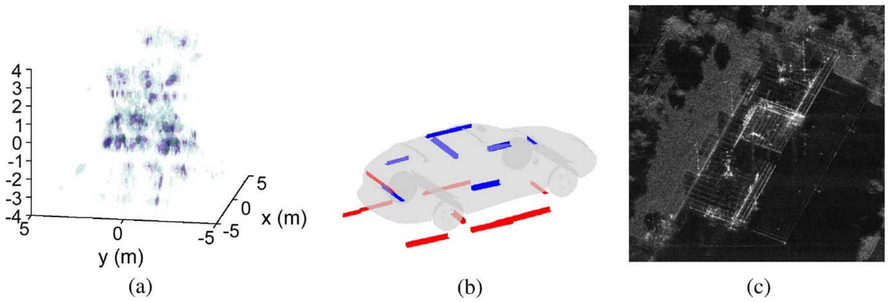

Fig. 1. *Radar images are compressible. (a) Matched filter three-dimensional image. (b) Nonlinear regression can yield a parsimonious representation of reflectors. (c) Radar image collected using MiniSAR demonstrating the compressibility of radar scenes.*

estimated model parameters for (three-dimensional) position, orientation, length (azimuth response), and polarization. For visualization, a faceted model of the actual vehicle is superimposed in the figure. The apparent points of reflection for the multipath contributions (even bounce polarization is shown in red) are along the dihedral crease formed by the intersecting planes of the asphalt surface and vehicle side panel.

Similarly, wide-area low-resolution images with many reflectors resident in each pixel are typically compressible in a suitable basis. In Fig. 1(c), the urban scene imaged using the MiniSAR system[1] can be transform encoded with 20 : 1 compression and less than 2% squared error. Image texture, especially shadow, can be critical for many inference problems; moreover, phase in the complex-valued image can reveal diffraction and closely spaced reflectors [22], [23]. Thus, radar images are compressible using either parametric models of physical scattering behaviors or transform coding.

B. Algorithms for Sparse Linear Regression

At least three classes of algorithms appear in both CS performance guarantees and existing radar applications. The algorithms may be viewed as attempts to exploit the sparsity, or compressibility, of the scene reflectivity in order to regularize an otherwise ill-posed linear inverse problem. The first class uses ℓ_p-norm regularization; the second class comprises fast greedy heuristics; and the third class uses iteratively reweighted ℓ_2 minimizations to approximate the ℓ_1 minimization. We briefly survey these three approaches.

First, linear inversion and deconvolution with ℓ_p-penalized least squares have a long history [24]–[26]. In this class of approaches, parameters are found via the optimization

$$\hat{\boldsymbol{f}} = \arg\min_{\boldsymbol{f}} \|\boldsymbol{A}\boldsymbol{f} - \boldsymbol{y}\|_2^2 + \lambda\|\boldsymbol{f}\|_p^p. \tag{17}$$

[1]http://www.sandia.gov/.

For $p \geq 1$, (17) is equivalent to the dual formulation in (2)

$$\hat{\boldsymbol{f}} = \arg\min_{\boldsymbol{f}} \|\boldsymbol{f}\|_p^p \text{ subject to } \|\boldsymbol{A}\boldsymbol{f} - \boldsymbol{y}\|_2^2 \leq \epsilon^2$$

for appropriate choice of λ. The large class of imaging methods adopting (17) may be interpreted as providing the Bayesian maximum posterior probability (MAP) estimate of $\boldsymbol{f}$ under a sparsity inducing prior [27]

$$p(\boldsymbol{f}) \propto \exp\left\{-\alpha\|\boldsymbol{f}\|_p^p\right\} \tag{18}$$

where $\lambda = 2\sigma^2\alpha$ and σ^2 denotes the variance of the assumed additive white Gaussian measurement noise. For $p = 1$, (17) is the convex relaxation of the minimum ℓ_0 problem; CS manuscripts have established sufficient conditions on the level of sparsity, noncoherence of the regressors, and number of measurements to ensure stable reconstruction, e.g., [1], [2], [4], [6], and [28]. For extension to $p < 1$, see [29].

The $p = 1$ regularization was advocated for radar imaging in [30]. Applications to radar imaging for $0 < p \leq 1$ and for a total variation norm on pixel magnitudes were introduced in [31], with extension to passive radar for multiple transmitters in [32]. The algorithm in [31] employs an approximate Hessian and uses conjugate gradients with a Toeplitz embedding of the Gram matrix $\boldsymbol{A}^H\boldsymbol{A}$; a majorization-minimization approach [33] yields the same iterative algorithm. Direct application of conjugate gradients to (17) was presented in [34].

A second class of algorithms contains various greedy approaches with low computational complexity. Greedy algorithms in array processing date at least to a heuristic iterative deconvolution algorithm known as CLEAN, which was introduced in 1974 [35] and is equivalent to matching pursuits [36]. Examples of subsequent variations for radar include frequency-dependent basis functions [30], [37] and a modified tree search [38]. Orthogonal matching pursuit (OMP) [39] typifies greedy approaches and comes with a guarantee of stable recovery [40] for suitably sparse $\boldsymbol{f}$ and $\boldsymbol{A}$ with suitably small mutual coherence. OMP successively selects from the $\boldsymbol{A}$ matrix the column $\boldsymbol{a}_n$ that is most highly correlated with the residual

$$\boldsymbol{y}_{\text{res}} = \boldsymbol{y} - \sum_{k=1}^{n-1} f_k \boldsymbol{a}_k$$

and updates the amplitude parameters $\{f_k\}_{k=1}^{n}$ via recursive least squares. From the CS literature, a variant of orthogonal matching pursuit CoSaMP that iteratively selects and then prunes a group of coefficients [41], [42] provides stronger performance guarantees for stable signal recovery. Thus, CS links the greedy heuristics to the convex relaxations and provides lower bounds on performance in terms of RICs (or mutual coherence), sparsity, and error norms.

Despite the performance guarantees established for greedy algorithms, a recent study [43] of moderately sized three-dimensional imaging ($N \sim 10^8$, $M \sim 10^4$) using measured airborne data [20] showed marked improvement of ℓ_1 over a greedy approach, OMP. Preliminary empirical results in this vein suggest that the penalized least squares approaches to solving sparse reconstruction problems may provide superior reconstruction performance compared to greedy approaches like CoSaMP and OMP for some classes of radar imaging problems.

A third class of sparse reconstruction algorithms appearing in both radar imaging and CS is iteratively reweighted linear least squares (IRLS) [44], [45]. As with the other algorithm classes, the IRLS approach has a long history, e.g., [46]–[48]. In this approach, a sequence of weighted ℓ_2 minimizations is used to solve the ℓ_1 minimization [49], [50]—and hence solve the ℓ_0 problem for suitably sparse $\boldsymbol{f}$ and $\boldsymbol{A}$ with suitably small RIC. In a similar vein, a sequence of weighted ℓ_1 minimizations may be used to approximate the ℓ_0 minimization [49], [51]; although this approach is, as yet, without a provable performance guarantee, numerical experiments suggest convergence to a sparse solution using fewer measurements and with greater computational cost than IRLS.

C. Coherence and Randomization

Randomization emerges from CS theory to provide a forward operator $\boldsymbol{A}$ with low RIC and low mutual coherence. In radar imaging, $\boldsymbol{A}$ is the combined result of transmit waveform and sensor geometry, and randomization has been employed for both waveforms and geometry.

Synthetic aperture radar may be viewed as an array processing task in which cross-range resolution is obtained by forming a directional beam pattern with the phased array of aperture locations; sidelobes appear due to correlation among responses from different directions. Randomization of array element locations has been studied as a means of reducing sidelobes in sparsely populated arrays [52]–[54]. A similar use of randomization for reduced imaging sidelobes has appeared in magnetic resonance tomographic imaging [55]. A strength of the compressed sensing results is that coherence of a linear model, characterized by a RIC or the mutual coherence, is linked to the conservative performance guarantees for specific inversion algorithms. This link is exploited, for example, in [16] and [56] to design pseudorandom spatial sampling patterns in multistatic radar to be used in conjunction with an ℓ_1-regularized least squares imaging algorithm.

Not only has spatial sampling of apertures been randomized but waveforms have, too, in "noise radar" to generate wide-band signals with nearly constant envelope [57]–[59]. Likewise, jittering, or staggering, of pulse repetition intervals has been used to randomize radar waveforms [7]. However, only recently have low-coherence properties been mated with ℓ_1-regularized or greedy reconstruction algorithms for sparse imaging; examples include random binary waveforms for recovery of one-dimensional range profiles [60], random phase waveforms for multistatic images [16], frequency-hopped measurements for ground penetrating radar images [61], and passive imaging using communications waveforms [62]. For the special case of range/Doppler processing for monostatic radar with a single pulse, the Alltop cubic-chirp sequence has been employed [63] as a deterministic construction of a low-coherence waveform; for prime length, the Alltop sequence nearly achieves the Welch bound on coherence, thus producing a nearly thumbtack ambiguity function with narrow peak and widely dispersed sidelobes. In recent CS literature, restricted isometry properties are established in [64] for observation matrices that exhibit structured statistical dependencies. We believe that present technology and radar modes of operation favor digital waveform generation as a means of pseudorandomization to achieve both good RICs and efficient operation of power amplifiers.

Thus, the two themes of sparse reconstruction algorithms and pseudorandomized data acquistion are longstanding concepts in radar processing; however, compressed sensing gives an easily accessible framework that illuminates the power of purposefully combining these two themes.

D. Spectrum Estimation

In Section III-B, we surveyed imaging algorithms appearing in both CS literature and radar applications. In addition to these algorithms, adaptive filter bank and subspace methods from spectrum estimation [65], [66] have been widely used in radar imaging to exploit sparsity.

The inner products computed in (11) may be interpreted as a bank of matched filters. Adaptive filter weights have been proposed as an apodization method to reduce speckle and sidelobes [67], [68]. For example, in [68], the filter weights at each image pixel are computed to minimize the least squares difference between the filtered data and an ideal point reflector, with a linear constraint of unity gain. Several similar adaptive filter banks are given in an extensive survey [69]. The algorithms adopt quadratic costs, therefore requiring estimates of data covariance matrices and typically using unweighted Fourier transform images as an intermediate step.

Subspace methods are applicable to radar imaging via a point-scattering assumption. In (14), the Fourier samples from a sparse scene of K point reflectors are sums of K complex exponentials. Subspace methods [69]–[72] assume rectangular Fourier sampling and exploit the property that complex exponentials are the homogeneous solutions to linear constant-coefficient difference equations. Computation entails singular-value decompositions and order-K polynomial rooting. The subspace methods can achieve the Cramèr–Rao lower bound on location error variance for the sum-of-reflectors model with sufficiently high signal-to-noise ratio [73].

Thus, spectrum estimation approaches directly exploit sparsity via a nonlinear parametric estimation approach, whereas the CS framework samples the unknown parameters to arrive at a sparse linear regression task. However, many factors limit the utility of spectrum estimation algorithms for radar imaging: the assumptions of uniform sampling and planar wavefronts, high levels of correlated clutter, order selection, and computational complexity.

IV. EXAMPLE APPLICATIONS

We briefly present example radar processing problems and results obtained using sparsity-driven reconstruction algorithms and CS concepts.

A. ℓ_p-Norms for Sparse Phase Coherent Imaging

Sparsity-driven reconstruction based on ℓ_p-norm constraints and their variants have been successfully used in radar imaging. Here, we provide an overview of these developments and display sample results. Generalizing (17), we have

$$\hat{\boldsymbol{f}} = \arg\min_{\boldsymbol{f}} \|\boldsymbol{A}\boldsymbol{f} - \boldsymbol{y}\|_2^2 + \lambda\|(L|\boldsymbol{f}|)\|_p^p \tag{19}$$

where $p \leq 1$. Two aspects of this modification are worth noting. First, we have included the possibility of using an operator L in the ℓ_p-norm constraint. When $\boldsymbol{f}$ is taken as the complex-valued reflection coefficients of idealized point reflectors, this operator allows one to impose sparsity on features computed from the reflectivity magnitudes rather than requiring the reflectivity to be sparse under some linear transform. For example, [31] considers the use of a discretized gradient operator for L, leading to a sparsity constraint on the spatial derivatives of the reflectivity magnitudes, indicating a preference for piecewise smooth fields. Such piecewise smoothness constraints have a long history in real-valued image restoration and reconstruction under various names, including edge-preserving regularization [27] and total variation restoration [74]. The second aspect is that we focus on features of the reflectivity magnitudes $|\boldsymbol{f}|$. This is based on the observation that the phases of the complex-valued reflectivities can be highly random and spatially uncorrelated. Hence, simplicity of the scene should be encoded through the sparsity of some features of the *magnitudes*. This nonlinearity makes the optimization problem for radar imaging considerably more challenging than commonly used linear sparse representation problems. Efficient algorithms matched to this problem structure have been developed [31], [75]. These algorithms are based on half-quadratic regularization [76] and can be viewed as quasi-Newton methods with a specific Hessian update scheme. Another interpretation is that the overall nonquadratic problem is turned into a series of quadratic problems, each efficiently solved using conjugate gradients.

The algorithms proposed in [31] and [75] have initially been used on conventional SAR sensing scenarios involving narrow angular apertures and observations over a contiguous band of frequencies. Sample results on the MSTAR data[2] are shown in Fig. 2(a) and (b) together with the conventional reconstructions. The result in (a) is based on imposing sparsity on the reflectivities directly, and suggests the potential of improving the resolvability of dominant scatterers. The result in (b) is based on imposing sparsity on reflectivity gradients and demonstrates the potential of suppressing artifacts such as speckle. Such improvements have been partially quantified in terms of feature extraction accuracy and object classification performance [77].

Another way to formulate the problem in (19) is to include a representation dictionary $\boldsymbol{\Psi}$ explicitly in the formulation: $|\boldsymbol{f}| = \boldsymbol{\Psi}\boldsymbol{\alpha}$, where $\boldsymbol{\alpha}$ denotes the representation coefficients and $|\boldsymbol{f}|$ admits a sparse representation in $\boldsymbol{\Psi}$. Now, introducing the notation $\boldsymbol{f} = \boldsymbol{\Phi}|\boldsymbol{f}|$, where $\boldsymbol{\Phi}$ is a diagonal matrix containing the unknown reflectivity phases. The problem becomes [78]

$$\hat{\boldsymbol{\alpha}}, \hat{\boldsymbol{\Phi}} = \arg\min_{\boldsymbol{\alpha},\Phi} \|\boldsymbol{A}\Phi\Psi\boldsymbol{\alpha} - \boldsymbol{y}\|_2^2 + \lambda\|\boldsymbol{\alpha}\|_p^p. \tag{20}$$

Given the freedom of choosing the overcomplete dictionary $\boldsymbol{\Psi}$, [78] demonstrates the use of a number of dictionaries in radar imaging including wavelets, the combination of spikes and edges, and dictionaries of various geometric shapes matched to the expected scene structure.

The benefits provided by sparsity-driven imaging are even greater in nonconventional sensing scenarios in which the sensing aperture or the data are sparse or

[2] http://www.mbvlab.wpafb.af.mil/public/sdms/datasets/mstar/.

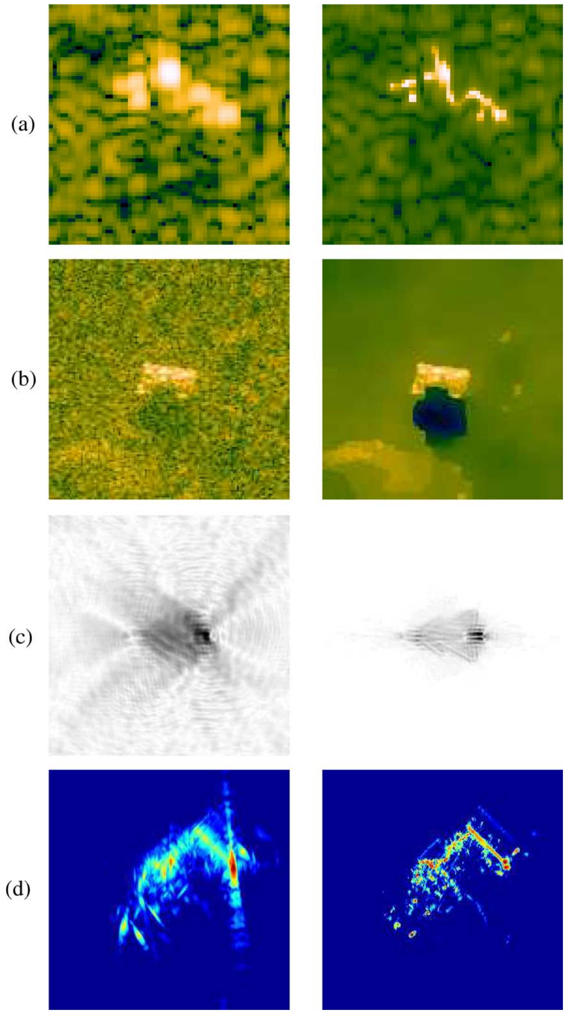

Fig. 2. *SAR imaging examples. (Left) Conventional imaging and (right) ℓ_p-norm-based reconstruction. (a) MSTAR example with sparsity imposed on reflection coefficients [31]. (b) MSTAR example with sparsity imposed on reflectivity gradients [31]. (c) Passive radar imaging example [32]. (d) Backhoe data (see https://www.sdms.afrl.af.mil/main.php) example for wide-angle imaging aperture of 110°.*

limited in some sense. Examples include multistatic passive sensing, data with frequency-band omissions, and three-dimensional imaging. Sparsity-driven imaging based on ℓ_p-norms has been extended to and applied in such scenarios [21], [32], [79], [80]. Sample results are shown in Fig. 2(c) and (d). The common observation is that sparsity-driven images exhibit fewer artifacts than conventional images.

B. Anisotropic Scattering

Isotropic point scattering is an idealized mathematical abstraction that becomes untenable for wide-angle apertures. Thus, wide-angle imaging invites reconstruction of scene reflectivity as a function of both position and viewing angle. Sparse reconstruction approaches have been offered for wide-angle imaging and differ in the assumed structure of scattering behavior versus azimuth angle.

The work in [79] and [80] assumes local isotropy and no further structure; an aperture is split into subapertures on which the isotropic scattering is assumed, and a sparse reconstruction is computed on each subaperture. The subaperture images are reported as either a sequence of angle-indexed images or as a single composite. Alternatively, angular dependence is assumed piece-wise constant in [81], leading to a mixed-norm version of (19): a total variation norm is applied in angle, and an ℓ_p norm is applied in the spatial dimensions.

In [82], an overcomplete dictionary is adopted within a sparse representation framework by assuming a sinc-like angular response and approximating it with a constant response over the main lobe. Thus, for each spatial location, the dictionary contains contiguous angular responses of prescribed extents and quantized center directions. For computational tractability, a tree structure of the dictionary is used to develop a fast greedy search. A sample result is shown in Fig. 3. The algorithm produces an estimate of the angular scattering function at each pixel of interest. Fig. 3(c) and (d) shows the selected azimuth responses at two particular pixels. The approach extends a generalized likelihood ratio test for sinc-like angular responses [83] to exploit the sparsity of bright reflectors.

C. Joint Sparsity

Many imaging radars use data from multiple channels; these can be SAR data collected at multiple elevations, multiple polarizations, multiple phase-centers, or multiple frequency bands. As before, the convolution of the point spread function gives rise to a linear model for each

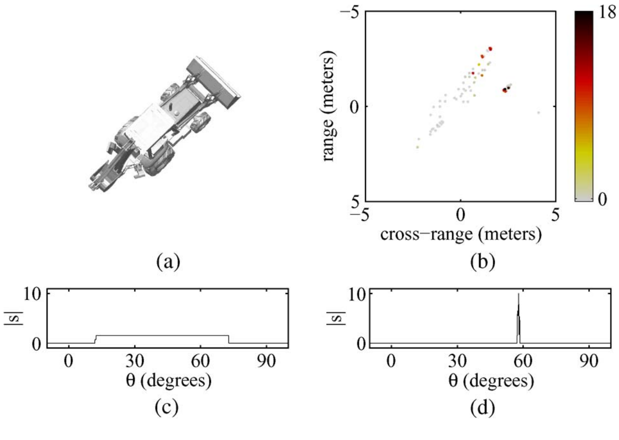

Fig. 3. *Joint imaging and angular anisotropy characterization through sparse representations based on the backhoe data. (a) Illustration of the scene. (b) 75 spatial locations of interest shaded according to maximum magnitude. (c) and (d) Aspect-dependent scattering solution for two example spatial locations. (Used with permission [82].)*

channel. In addition, the channels carry common information about the imaged scene. As an example, the different channels can share common support of sparsity or common edges of high contrast. In the special cases of interferometric SAR (IFSAR) and polarimetric SAR, precise relations between the channels can be imposed, such as having identical magnitude scatterers in the reconstructed images for the case of IFSAR, where the phase encodes the height information about the detected scatterers [10]. Sparse reconstruction techniques that process the images independently may lead to poor phase information between the channels [84]. In [85], a joint reconstruction method was proposed where the multiple channel ℓ_p-norm-based reconstruction is augmented by constraint functions that relate the reconstructed reflectivities. Specifically, for data collected across M channels

$$\hat{\boldsymbol{f}} = \arg\min_{\boldsymbol{f}} \sum_{i=1}^{M} \|\boldsymbol{A}_i \boldsymbol{f}_i - \boldsymbol{y}_i\|_2^2 + \lambda \|(L|\boldsymbol{f}_i|)\|_p^p,$$

$$\text{such that } \sum_{i=1}^{M} h_{ij}(\boldsymbol{f}_i) = 0 \text{ for } j = 1, \ldots N. \quad (21)$$

The nonlinear constraints $h_{ij}(\boldsymbol{f}_i)$ encode the common information between the multiple channels. For example, IFSAR applications require common magnitude constraints for the reflectivity coefficients, resulting in $N-1$ constraints of the form $|f_1| = |f_2| = \ldots = |f_N|$. Alternatively, for multiband frequency or polarimetric reconstructions, the constraints can be relaxed, requiring only $h(|f_1|) = h(|f_2|) = \ldots = h(|f_N|)$, with a sigmoidal $h(\cdot)$ constraining high amplitude reflectors to occupy the same resolution cells across the images. The joint optimization problem in (21) can be converted into an equivalent unconstrained problem through Lagrange multipliers [85]. The unconstrained problem can be solved efficiently using a dual descent method, which alternates between descent in the Lagrange multipliers and M independent optimization problems for each channel for a given set of channel weights. Although prior work focused on the multichannel enhancement of data, where the channels represent data from separate sensors, joint sparsity ideas could be applied to reconstruction of images at multiple resolutions. This line of research has been considered in recent work [86], [87].

A circular SAR (CSAR) data collection experiment conducted by the Air Force Research Laboratory [20], [21] features eight complete circular passes collected at an altitude of 25 000 ft at nominal 45° elevation angle using an airborne fully polarimetric SAR sensor. To illustrate the performance of the ℓ_p-norm regularized construction of radar imagery, we divided the data into 72 nonoverlapping windows of width $\Delta = 5°$ centered at $\phi_m \in \{0°, 5°, \ldots, 355°\}$ and used the entire 640 MHz bandwidth centered at 9.6 GHz for the single VV polarization. For returns from a stationary vehicle in the scene, Fig. 4(a) shows the phase noncoherent sum of the traditional Fourier-based images from a single pass. The Fourier-based image was enhanced using the ℓ_p-norm-based optimization problem given in (19). Fig. 4(b) and (c) shows the results for $p = 1.0$ and $p = 0.8$, respectively. The ℓ_p-norm-based regularization can also be applied to three-dimensional imagery if multiple elevation passes are available [88]–[90]. Fig. 5(a) and (b) shows traditional and sparsity-regularized reconstruction of the vehicle from eight circular passes.

Alternatively, (2-D) images from these eight passes could be jointly enhanced using joint sparsity constraints by solving the constrained optimization problem in (21). The resulting images share the same support but differ in their phases. The sum magnitude over the eight passes is given in Fig. 6 for independent and joint enhancement techniques for $p = 1.0$. We observe that joint processing

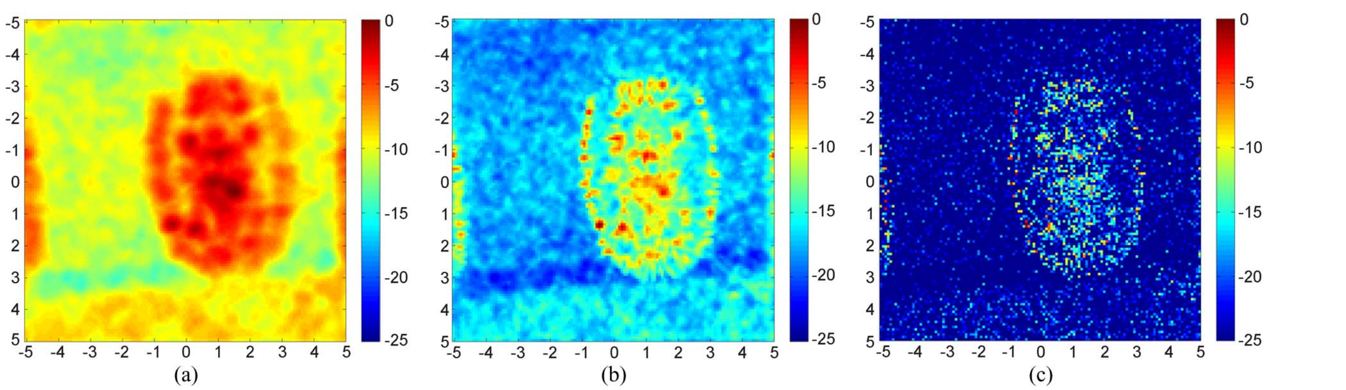

Fig. 4. ***SAR images of a vehicle from 360° aperture. (a) Standard Fourier image, sparsity regularized reconstruction using (b) $p = 1.0$ and (c) $p = 0.8$.***

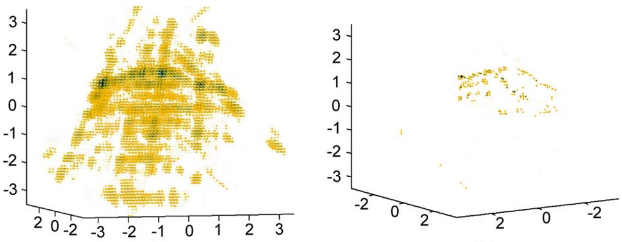

Fig. 5. ***Three-dimensional SAR images of a vehicle from eight passes with 360° aperture. (a) Standard Fourier image and (b) sparsity regularized reconstruction using $p = 0.8$.***

reduces clutter levels and provides better isolation of target features.

D. UNB Moving Target Indication

In this example, we describe an approach to radar that blends SAR and moving target indication (MTI) while simultaneously eliminating the need for high bandwidth waveforms. Specifically, a constellation of ultra-narrowband (UNB) sensors is used in a multistatic fashion to estimate both the positions and velocities of moving targets. A similar problem formulation was termed the "tomography of moving targets" in [91] and shown to be a special case of more general imaging techniques in [12]. Here, we demonstrate a greedy sparse reconstruction approach using CoSaMP; a similar formulation with ℓ_1-penalized least squares computation is given in [92].

A traditional wide-bandwidth monostatic SAR collects data densely sampled on an annular region in Fourier space characterized by (14). This densely sampled data is suitable for analysis with continuous methods and leads to familiar reconstruction techniques such as filtered backprojection, omega-k [93], polar format, and others [10].

In contrast, spatially distributed UNB sensors produce a cloud of sparsely sampled and widely dispersed points in Fourier space. Each transmitter emits a simple tone, which produces a single Fourier space sample for each listening receiver, with the Fourier locations governed by (15). Irregular spacing of the sensors can further accentuate this pseudorandom quality of the Fourier space measurement locations. The transmitters can either be multiplexed in time or use different transmit frequencies. In this way, a small set of tone waveforms can be used to obtain a set of pseudorandom projections of the scene's reflectivity, which are reasonably incoherent due to the geometric diversity of the sensor constellation. An analogy can be made to CS matrices that use random subsets of the columns of Fourier matrices [28].

The stop-and-hop assumption can be applied to ignore target motion during a single pulse. A sequence of such pulses can be used to obtain a model in the form (16). There are at most $P\sum_{k=1}^{S} k$ measurements for P pulses and S sensors. Each column of $\boldsymbol{A}$ will encode these measurements for one assumed initial position and velocity pair, corresponding to an element of $\boldsymbol{f}$.

The stationary background, i.e., clutter, can be removed either by subtracting background reference data or through adaptive nulling techniques in the spirit of space-time adaptive processing (STAP) [9], [94], [95]. Techniques to combine STAP and SAR are on ongoing areas of research [96]. Once the background has been removed, moving targets are sparse in the velocity/position domain.

We simulated a two-dimensional example using a constellation of 15 sensors placed along a 1 km radius ring. The exact positions were slightly perturbed from a perfect circle to promote reduced mutual coherence in the resulting dictionary. Monochromatic measurements at a frequency of 100 MHz were simulated for a pulse repetition frequency of 50 Hz. A square 2-D scene with an edge length of 100 m was placed at the center of the sensor ring, discretized into 1 m^2 pixels. The velocity was discretized to

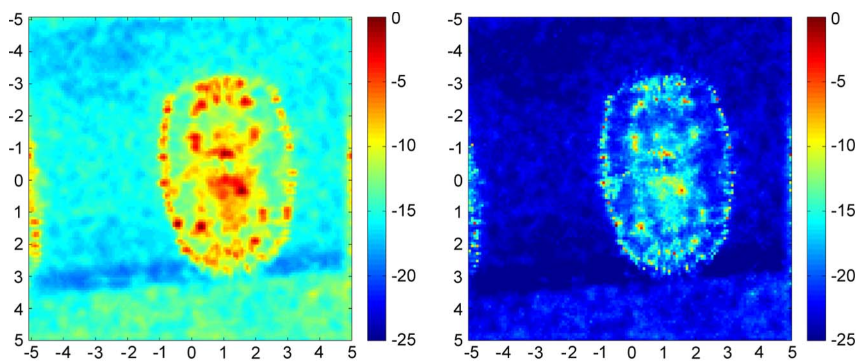

Fig. 6. ***Phase noncoherent sum of multichannel SAR images of a vehicle from eight passes with 360° aperture. (a) Independent enhancement and (b) joint enhancement.***

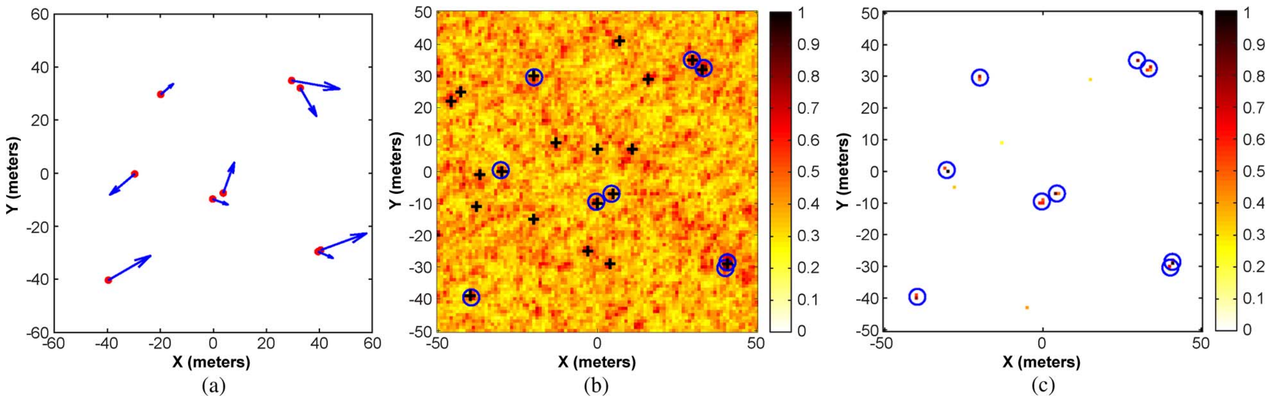

Fig. 7. ***Results for a moving targets example. (a) Truth data with red dots indicating initial target positions and blue arrows indicating constant linear velocities. (b) Matched filter reconstruction; true target locations are shown with blue circles. Black crosses indicate the top 20 local maxima. (c) The CoSaMP reconstruction. The blue circles indicate the true locations of the targets.***

include components in each dimension ranging from −35 to 35 m/s in 5.0 m/s steps. The resulting $\boldsymbol{A}$ matrix is 960 by 2 295 225 elements.

A collection of nine targets was simulated, each with unit amplitude and a speed of either 10, 20, or 30 m/s. The target configuration is shown in Fig. 7(a) with arrows indicating the direction and magnitude of the target velocities. All target positions and velocities were chosen to lie off the reconstruction grid points. Additive white Gaussian noise was also included to obtain an SNR of 25 dB.

CoSaMP was used to reconstruct the scene with 120 iterations and an assumed sparsity of 20, which is more than twice the true value. The simulation result is shown in Fig. 7(c). This figure was computed by taking the maximum reflectivity observed over all possible velocity choices for each pixel. For comparison, the matched filter reconstruction is shown in Fig. 7(b). The top 20 local maxima are marked with black crosses to illustrate simple target detections using this ℓ_2 approach. A single target is missed due to its proximity to another target, while several false alarms appear. Table 1 shows the estimated velocities using CoSaMP, which closely match the simulated values. The velocity estimates are derived from the maximum coefficient in the reconstruction associated with the pixel closest to each target. In the example, CoSaMP is able to accurately estimate both the positions and velocities of the targets without introducing excessive false alarms. Bias due to grid sampling dominates the reconstruction error.

V. DISCUSSION

A. Practice Motivating Theory

The influence of compressed sensing in radar remains an unfolding story. CS theorems sprang from the curiously successful empirical results from long-standing ad hoc sparse recovery algorithms. In this sense, future advances in CS theory may similarly arise from the successes of other ad hoc processing procedures from radar or other application domains. We consider five example potential directions.

Table 1 Target Positions (x, y), Actual Velocities (v_x, v_y), Velocity Estimates $(\hat{v}_x, \hat{v}_y)$, and Velocity Error Norms $\|v - \hat{v}\|_2$ for the Moving Targets Example. Results Are in Meters and Meters per Second. Estimates Are Based on the CoSaMP Reconstruction

x	y	v_x	v_y	$\hat{v}_x$	$\hat{v}_y$	$\|\boldsymbol{v}-\hat{\boldsymbol{v}}\|_2$
-39.69	-39.59	25.98	15.00	30.00	20.00	6.42
-30.37	0.41	-15.32	-12.86	-20.00	-10.00	5.48
-19.87	29.60	7.66	6.43	10.00	5.00	2.74
29.78	35.05	29.54	-5.21	25.00	-5.00	4.55
33.46	32.46	10.00	-17.32	15.00	-15.00	5.51
-0.34	-9.53	9.40	-3.42	5.00	5.00	9.50
4.46	-7.01	6.84	18.79	10.00	20.00	3.38
40.30	-30.36	9.21	-3.91	10.00	-5.00	1.35
40.92	-28.58	28.19	10.26	25.00	15.00	5.71

First, sparse linear regression entails sampling the parameters (such as spatial location), which results in biased estimates. Common processing approaches to reduce bias are to use iterative grid refinement or to compute the (nonconvex) maximum likelihood parametric estimate using an initialization from the linear regression [19], [97]. Indeed, grid refinement has been employed to expand the dictionary for all three algorithm classes surveyed in Section III-B [98]–[100]. An open question is to characterize the bias and variance of greedy or ℓ_1 algorithms as estimators for an underlying, continuous-valued parameter set.

A second, and related, example candidate stems from the good empirical results observed with highly coherent dictionaries [43], [61]. For inverse problems, the columns of the linear model $\boldsymbol{A}$ in (16) typically arise from sampling a continuous parameter space, e.g., spatial location, and the topology of the parameter space is lost in the linear regression model. Resolution is the ability to detect two objects in close proximity [73], [101], [102], while accuracy refers to the mean squared error in estimating the object's parameters (location, amplitude, etc.). The suppression of image sidelobes by ℓ_1 or greedy algorithms may invite a qualitative claim of "superresolution"; however, existing CS results are silent regarding resolution and agnostic regarding bias and variance of parameter estimates in the underlying continuous parameter space. Indeed, superresolution implies that mutual coherence must be large. Can sufficient conditions for stable recovery be extended to provide modified performance guarantees for coherent dictionaries and well-separated reflectors? Recent empirical results [103] suggest that ℓ_p-penalized least squares, for $p \leq 1$, performs as well or better than subspace methods for high-resolution range profiles estimated from limited bandwidth waveforms. For a limited bandwidth and high-resolution spatial sampling in the reconstruction, the mutual coherence of the resulting linear model $\boldsymbol{A}$ is very large, irrespective of waveform randomization.

A third candidate direction is the expansion of notions of sparsity and structure [104]; for example, a total variation norm on the magnitude of a complex image [31] does not tidily fit within existing frameworks. A fourth direction is the joint estimation of both the unknowns $\boldsymbol{f}$ and a parametric model of uncertainty in $\boldsymbol{A}$. An important example in radar imaging is autofocus, whereby antenna locations at each pulse are estimated to subwavelength accuracy. The approach is adopted in [105], where phase errors are included as nuisance parameters in the ℓ_p-regularized optimization problem (19). A fifth potential direction is the adoption of Bayesian priors, other than (18), to exploit sparsity when coherence or noise may create significant ambiguity among candidate sparse solutions. For example, [106] and [107] consider a Bayes model averaging approach whereby a minimum mean squared error reconstruction, in contrast to a MAP solution, is approximately computed as a weighted sum of sparse solutions. For candidate sparse solutions, the fast greedy search in [106] provides exact ratios of posterior probabilities given the noisy measurements.

B. Theory Motivating Practice

Is CS merely a transient bandwagon [108] of little lasting relevance for radar applications? Time will tell; but we speculate that CS is relevant to radar imaging for five reasons.

1) The algorithms admitting performance guarantees in CS are established techniques in radar imaging; greedy algorithms and ℓ_p regularization have a long history in radar processing that is likely to continue. CS informs and encourages refinement (e.g., [41]) of these algorithmic approaches.
2) Coherence likewise has a prominent and physically interpretable place in the radar imaging literature, in the form of the radar ambiguity function.
3) Importantly, CS invites provable performance guarantees for any proposed sparse imaging algorithm, just as CS provides sufficient conditions on sparsity and coherence to achieve stable recovery.
4) CS explicitly characterizes low-coherence acquisition schemes as well-mated to specific nonlinear reconstruction algorithms. Thus, CS gives an accessible framework that serves as an impetus to consider nonconventional data-acquisition schemes.
5) CS is consistent with the digital technology trend that encourages a tradeoff of reduced acquisition complexity in exchange for increased processing complexity, in the form of nonlinear reconstruction. Likewise, digital technology allows for low-cost flexibility in waveform generation with the aim of low coherence in the data model $\boldsymbol{A}$.

Thus, for these reasons, we speculate that compressed sensing will serve as a catalyst for future developments in radar imaging. ■

REFERENCES

[1] E. Candès, J. Romberg, and T. Tao, "Stable signal recovery from incomplete and inaccurate measurements," *Commun. Pure Applied Math.*, vol. 59, no. 8, pp. 1207–1223, 2006.

[2] D. L. Donoho, "Compressed sensing," *IEEE Trans. Inf. Theory*, vol. 52, pp. 1289–1306, Apr. 2006.

[3] E. Candès, "The restricted isometry property and its implications for compressed sensing," *Comptes rendus-Math.*, vol. 346, no. 9–10, pp. 589–592, 2008.

[4] J. A. Tropp, "Just relax: Convex programming methods for identifying sparse signals in noise," *IEEE Trans. Inf. Theory*, vol. 51, pp. 1030–1051, Mar. 2006.

[5] M. A. Herman and T. Strohmer, "General deviants: An analysis of perturbations in compressed sensing," *IEEE J. Sel. Topics Signal Process. (Special Issue on Compressive Sensing)*, to be published.

[6] D. L. Donoho, M. Elad, and V. N. Temlyakov, "Stable recovery of sparse overcomplete representations in the presence of noise," *IEEE Trans. Inf. Theory*, vol. 52, pp. 6–18, Jan. 2006.

[7] M. Skolnik *et al., RADAR Handbook*. New York: McGraw-Hill, 2008.

[8] M. Richards, *Fundamentals of Radar Signal Processing*. New York: McGraw-Hill, 2005.

[9] J. Guerci, *Space-Time Adaptive Processing for Radar*. Norwood, MA: Artech House, 2003.

[10] C. V. Jakowatz *et al.*, *Spotlight-Mode Synthetic Aperture Radar: A Signal Processsing Approach*. New York: Springer, 1996.
[11] M. Soumekh, *Synthetic Aperture Radar Signal Processing With MATLAB Algorithms*. New York: J. Wiley, 1999.
[12] M. Cheney and B. Borden, "Imaging moving targets from scattered waves," *Inverse Prob.*, vol. 24, no. 3, p. 035005, 2008.
[13] D. C. Munson, Jr., J. D. O'Brien, and W. K. Jenkins, "A tomographic formulation of spotlight-mode synthetic aperture radar," *Proc. IEEE*, vol. 71, pp. 917–925, Aug. 1983.
[14] O. Arikan and D. C. Munson, Jr., "A tomographic formulation of bistatic synthetic aperture radar," in *Proc. ComCon*, Oct. 1988.
[15] B. Rigling, *Advances in Bistatic Radar*. Raleigh, NC: Scitech, 2007, pp. 320–431.
[16] N. S. Subotic, B. Thelen, K. Cooper, W. Buller, J. Parker, J. Browning, and H. Beyer, "Distributed RADAR waveform design based on compressive sensing considerations," in *Proc. IEEE Radar Conf.*, May 2008, pp. 1–6.
[17] J. B. Keller, "Geometrical theory of diffraction," *J. Opt. Soc. Amer.*, vol. 5, no. 2, pp. 116–130, 1962.
[18] M. J. Gerry, L. C. Potter, I. J. Gupta, and A. van der Merwe, "A parametric model for synthetic aperture radar measurements," *IEEE Trans. Antennas Propag.*, vol. 47, pp. 1179–1188, Jul. 1999.
[19] J. A. Jackson, B. D. Rigling, and R. L. Moses, "Canonical scattering feature models for 3D and bistatic SAR," *IEEE Trans. Aerosp. Electron. Syst.*, to be published.
[20] C. H. Casteel, Jr., L. A. Gorham, M. J. Minardi, S. M. Scarborough, K. D. Naidu, and U. K. Majumder, "A challenge problem for 2D/3D imaging of targets from a volumetric data set in an urban environment," in *Proc. SPIE Algorithms Synthetic Aperture Radar Imagery XIV*, Apr. 2007, vol. 6568.
[21] E. Ertin, C. D. Austin, S. Sharma, R. L. Moses, and L. C. Potter, "GOTCHA experience report: Three-dimensional SAR imaging with complete circular apertures," in *Proc. SPIE Algorithms Synthetic Aperture Radar Imagery XIV*, Apr. 2007, vol. 6568.
[22] B. Rigling, "Physics, Fisher and phase: Information content in SAR images," master's thesis, The Ohio State University, Columbus, 2000.
[23] A. Rihaczek and S. Hershkowitz, "Man-made target backscattering behavior: Applicability of conventional radar resolution theory," *IEEE Trans. Aerosp. Electron. Syst.*, vol. 32, pp. 809–824, Apr. 1996.
[24] A. N. Tikhonov and V. Y. Arsenin, *Solutions of Ill-Posed Problems*. Washington, DC: Winston, 1977.
[25] A. E. Hoerl and R. W. Kennard, "Ridge regression: Biased estimation for nonorthogonal problems," *Technometrics*, vol. 12, pp. 55–67, Feb. 1970.
[26] H. L. Taylor, S. C. Banks, and J. F. McCoy, "Deconvolution with the ℓ_1 norm," *Geophysics*, vol. 44, no. 1, pp. 39–52, 1979.
[27] C. Bouman and K. Sauer, "A generalized Gaussian image model for edge-preserving MAP estimation," *IEEE Trans. Image Process.*, vol. 2, pp. 296–310, Mar. 1993.
[28] E. Candès, J. Romberg, and T. Tao, "Robust uncertainty principles: Exact signal reconstruction from highly incomplete frequency information," *IEEE Trans. Inf. Theory*, vol. 52, pp. 489–509, Feb. 2006.
[29] R. Chartrand and V. Staneva, "Restricted isometry properties and nonconvex compressive sensing," *Inverse Prob.*, vol. 24, no. 035020, pp. 1–14, 2008.
[30] J. W. Burns, N. S. Subotic, and D. Pandelis, "Adaptive decomposition in electromagnetics," in *Proc. Int. Symp. Antennas Propag. Soc.*, Jul. 1997, pp. 1984–1987.
[31] M. Çetin and W. C. Karl, "Feature-enhanced synthetic aperture radar image formation based on nonquadratic regularization," *IEEE Trans. Image Process.*, vol. 10, pp. 623–631, Apr. 2001.
[32] M. Çetin and A. Lanterman, "Region-enhanced passive radar imaging," *Proc. Inst. Elect. Eng. Radar, Sonar Navig.*, vol. 152, pp. 185–194, Jun. 2005.
[33] T. J. Kragh and A. A. Kharbouch, "Monotonic iterative algorithms for SAR image restoration," in *Proc. IEEE Int. Conf. Image Process.*, Oct. 2006, pp. 645–648.
[34] A. H. Delaney and Y. Bresler, "A fast and accurate Fourier algorithm for iterative parallel-beam tomography," *IEEE Trans. Image Process.*, vol. 5, pp. 740–753, May 1996.
[35] J. Høgbom, "Aperture synthesis with a non-regular distribution of interferometer baselines," *Astrophys. Astrophys. Suppl. Series*, vol. 15, pp. 417–426, 1974.
[36] S. Mallat and Z. Zhang, "Matching pursuits with time-frequency dictionaries," *IEEE Trans. Signal Process.*, vol. 41, pp. 3397–3415, Dec. 1993.
[37] M. R. McClure and L. Carin, "Matching pursuits with a wave-based dictionary," *IEEE Trans. Signal Proces.*, vol. 45, pp. 2912–2927, Dec. 1997.
[38] R. Bose, A. Freedman, and B. Steinberg, "Sequence CLEAN: A modified deconvolution technique for microwave images of contiguous targets," *IEEE Trans. Aerosp. Electron. Syst.*, vol. 38, pp. 89–97, Jan. 2002.
[39] Y. C. Pati, R. Rezaiifar, and P. S. Krishnaprasad, "Orthogonal matching pursuit: Recursive function approximation with applications to wavelet decomposition," in *Proc. 27th Annu. Asilomar Conf. Signals, Syst., Comput.*, Nov. 1993, pp. 40–44.
[40] J. Tropp, "Greed is good: Algorithmic results for sparse approximation," *IEEE Trans. Inf. Theory*, vol. 50, pp. 2231–2242, Oct. 2004.
[41] D. Needell and J. A. Tropp, "CoSaMP: Iterative signal recovery from incomplete and inaccurate samples," *Appl. Comput. Harmon. Anal.*, vol. 26, pp. 301–321, 2008.
[42] W. Dai and O. Milenkovic. Subspace pursuit for compressive sensing: Closing the gap between performance and complexity, Mar. 2008, arXiv:0803.0811v3
[43] M. Ferrara, J. Jackson, and M. Stuff, "Three-dimensional sparse-aperture moving-target imaging," in *Proc. SPIE Algorithms Synthetic Aperture Radar Imagery XIV*, Mar. 2008, vol. 6970, p. 697006.
[44] S. D. Cabrera, B. C. Flores, E. Rodriguez, and G. Thomas, "Two-dimensional extrapolation and spectral estimation from arbitrary sampling configurations for SAR/ISAR imaging," in *Proc. 28th Asilomar Conf. Signals, Syst. Comput.*, Oct. 1994, pp. 145–150.
[45] A. E. Brito, S. H. Chan, and S. D. Cabrera, "SAR image formation using 2D reweighted minimum norm extrapolation," in *Proc. SPIE Algorithms Synthetic Aperture Radar Imagery VI*, 1999, vol. 3721, pp. 78–91.
[46] C. L. Lawson, "Contributions to the theory of linear least maximum approximations," Ph.D. dissertation, Univ. California, Los Angeles, 1961.
[47] H. Lee, D. Sullivan, and T. Huang, "Improvement of discrete band-limited signal extrapolation by iterative subspace modification," in *Proc. IEEE Int. Conf. Acoust., Speech Signal Process.*, Apr. 1987, vol. 12, pp. 1569–1572.
[48] B. D. Rao and K. Kreutz-Delgado, "An affine scaling methodology for best basis selection," *IEEE Trans. Signal Process.*, vol. 47, pp. 187–200, Jan. 1999.
[49] D. P. Wipf and S. Nagarajan, "Solving sparse linear inverse problems: Analysis of reweighted ℓ_1 and ℓ_2 methods," in *Proc. Workshop Signal Process. Adaptive Sparse Structured Represent.*, Apr. 2009.
[50] I. Daubechies, R. DeVore, M. Fornasier, and S. Gunturk, "Iteratively re-weighted least squares minimization for sparse recovery," *Commun. Pure Appl. Math.*, vol. 14, pp. 877–905, Dec. 2009.
[51] E. Candès, M. Wakin, and S. Boyd, "Enhancing sparsity by reweighted ℓ_1 minimization," *J. Fourier Anal. Applicat.*, vol. 14, pp. 877–905, Dec. 2008.
[52] Y. T. Lo, "A mathematical theory of antenna arrays with randomly spaced elements," *IEEE Trans. Antennas Propag.*, vol. AP-12, pp. 257–268, 1964.
[53] H. Unz, "Linear arrays with arbitrarily distributed elements," *IRE Trans. Antennas Propag.*, vol. AP-8, pp. 222–223, Mar. 1960.
[54] R. F. Harrington, "Sidelobe reduction by nonuniform element spacing," *IRE Trans. Antennas Propag.*, vol. AP-9, pp. 187–192, Mar. 1961.
[55] G. Marseille, R. De Beer, M. Fuderer, A. Mehlkopf, and D. Van Ormondt, "Nonuniform phase-encode distributions for MRI scan time reduction," *J. Magn. Res. B*, vol. 111, no. 1, pp. 70–75, 1996.
[56] I. Stojanovic, W. C. Karl, and M. Çetin, "Compressed sensing of mono-static and multi-static SAR," in *Proc. Algorithms Synthetic Aperture Radar Imagery XVI*, Apr. 2009, SPIE.
[57] B. Horton, "Noise-modulated distance measuring systems," *Proc. IRE*, vol. 47, pp. 821–828, May 1959.
[58] D. F. Albanese and A. M. Klein, *Pseudorandom code waveform design for CW radar*vol. AES-15, pp. 67–75, Jan. 1979.
[59] S. Axelsson, "Noise radar using random phase and frequency modulation," *IEEE Trans. Geosci. Remote Sens.*, vol. 42, pp. 2370–2384, Nov. 2004.
[60] R. Baraniuk and P. Steeghs, "Compressive radar imaging," in *Proc. IEEE 2007 Radar Conf.*, Apr. 2007, pp. 128–133.
[61] C. Gurbuz, J. McClellan, and R. Scott, Jr., "A compressive sensing data acquisition and imaging method for stepped frequency GPRs," *IEEE Trans. Signal Process.*, vol. 57, pp. 2640–2650, Jul. 2009.
[62] C. Berger, S. Zhou, and P. Willett, "Signal extraction using compressed sensing for passive radar with OFDM signals," in *Proc. 11th Int. Conf. Inf. Fusion*, Jun. 2008, pp. 1–6.
[63] M. A. Herman and T. Strohmer, "High-resolution radar via compressed sensing," *IEEE Trans. Signal Process.*, vol. 57, pp. 2275–2284, Jun. 2009.
[64] J. Haupt, W. U. Bajwa, G. Raz, and R. Nowak, "Toeplitz compressed sensing matrices with applications to sparse channel estimation," submitted for publication.
[65] P. Stoica and R. Moses, *Spectral Estimation of Signals*. Englewood Cliffs, NJ: Prentice-Hall, 2005.
[66] J. McClellan, "Multidimensional spectral estimation," *Proc. IEEE*, pp. 1029–1039, Sep. 1982.
[67] G. R. Benitz, "High-definition vector imaging," *Lincoln Lab. J.*, vol. 10, no. 2, pp. 147–170, 1997.

[68] P. Stoica, H. Li, and J. Li, "A new derivation of the APES filter," *IEEE Signal Process. Lett.*, pp. 205–206, Aug. 1999.

[69] S. R. DeGraaf, "SAR imaging via modern 2-D spectral estimation methods," *IEEE Trans. Image Process.*, vol. 7, pp. 729–761, May 1998.

[70] S. Y. Kung, K. S. Arun, and D. V. B. Rao, "State-space and singular-value decomposition-based approximation methods for the harmonic retrieval problem," *J. Opt. Soc. Amer.*, vol. 73, pp. 1799–1811, Dec. 1983.

[71] B. Rao and K. Arun, "Model based processing of signals: A state space approach," *Proc. IEEE*, vol. 80, pp. 283–309, Feb. 1992.

[72] Y. Hua, F. Baqai, Y. Zhu, and D. Heilbronn, "Imaging of point scatterers from step-frequency ISAR data," *IEEE Trans. Aerosp. Electron. Syst.*, vol. 29, pp. 195–205, Jan. 1993.

[73] T. Blu, P.-L. Dragotti, M. Vetterli, P. Marziliano, and L. Coulot, "Sparse sampling of signal innovations," *IEEE Signal Process. Mag.*, pp. 31–40, Mar. 2008.

[74] L. I. Rudin, S. Osher, and E. Fatemi, "Nonlinear total variation based noise removal algorithms," *Phys. D*, vol. 60, no. 5, pp. 259–268, 1992.

[75] M. Çetin, W. C. Karl, and A. S. Willsky, "Feature-preserving regularization method for complex-valued inverse problems with application to coherent imaging," *Opt. Eng.*, vol. 45, pp. 017003 1–017003 11, Jan. 2006.

[76] D. Geman and C. Yang, "Nonlinear image recovery with half-quadratic regularization," *IEEE Trans. Image Process.*, vol. 4, pp. 932–946, Jul. 1995.

[77] M. Çetin, W. C. Karl, and D. A. Castañón, "Feature enhancement and ATR performance using non-quadratic optimization-based SAR imaging," *IEEE Trans. Aerosp. Electron. Syst.*, vol. 39, pp. 1375–1395, Oct. 2003.

[78] S. Samadi, M. Çetin, and M. A. Masnadi-Shirazi, "Multiple feature-enhanced synthetic aperture radar imaging," in *Proc. SPIE Algorithms Synthetic Aperture Radar Imagery XVI*, Apr. 2009, vol. 7337, pp. 73370I 1–73370I 10.

[79] R. L. Moses, L. Potter, and M. Çetin, "Wide angle SAR imaging," in *Proc. SPIE Algorithms Synthetic Aperture Radar Imagery XI*, Apr. 2004.

[80] M. Çetin and R. L. Moses, "SAR imaging from partial-aperture data with frequency-band omissions," in *Proc. SPIE Algorithms Synthetic Aperture Radar Imagery XII*, Mar./Apr. 2005, vol. 5808, pp. 32–43.

[81] I. Stojanovic, M. Çetin, and W. C. Karl, "Joint space aspect reconstruction of wide-angle sar exploiting sparsity," in *Proc. SPIE Defense Security Symp. Algorithms Synthetic Aperture Radar Imagery XV*, 2008.

[82] K. R. Varshney, M. Çetin, J. W. Fisher, III, and A. S. Willsky, "Sparse signal representation in structured dictionaries with application to synthetic aperture radar," *IEEE Trans. Signal Process.*, vol. 56, pp. 3548–3561, Aug. 2008.

[83] M. R. Allen, J. M. Jauregui, and L. E. Hoff, "FOPEN-SAR detection by direct use of simple scattering physics," in *Proc. SPIE Algorithms Synthetic Aperture Radar Imagery II*, Apr. 1995, vol. 2487.

[84] N. Ramakrishnan, E. Ertin, and R. L. Moses, "Joint enhancement of multichannel SAR data," in *Proc. SPIE Algorithms Synthetic Aperture Radar Imagery XIV*, Apr. 2007, pp. 6568.

[85] N. Ramakrishnan, E. Ertin, and R. L. Moses, "Enhancement of coupled multichannel images using sparsity constraints," submitted for publication.

[86] M. Fornasier and H. Rauhut, "Recovery algorithms for vector-valued data with joint sparsity constraints," *SIAM J. Numer. Anal.*, vol. 46, no. 2, pp. 577–613, Mar. 2008.

[87] M. Duarte, M. Wakin, and R. Baraniuk, "Wavelet-domain compressive signal reconstruction using a hidden Markov tree model," in *Proc. IEEE Int. Conf. Acoust., Speech, Signal Process.*, 2008, pp. 5137–5140.

[88] E. Ertin, L. Potter, and R. Moses, "Enhanced imaging over complete circular apertures," in *Proc. 40th Annu. Asilomar Conf. Signals, Syst. Comput.*, 2006, pp. 1580–1584.

[89] C. D. Austin and R. L. Moses, "Wide-angle sparse 3D synthetic aerture radar imaging for nonlinear flight paths," in *Proc. IEEE Nat. Aerosp. Electron. Conf.*, 2008, pp. 330–336.

[90] C. Austin, E. Ertin, and R. L. Moses, "Sparse multipass 3D imaging: Applications to the GOTCHA data set," in *Proc. SPIE Defense Security Symp. Algorithms Synthetic Aperture Radar Imagery XVI*, 2009, vol. 7337, p. 733703-1–733703-12.

[91] B. Himed, H. Bascom, J. Clancy, and M. C. Wicks, "Tomography of moving targets (TMT)," in *Proc. SPIE Sensors, Syst., Next-Gen. Satellites V*, 2001, vol. 4540, pp. 608–619.

[92] I. Stojanovic and W. C. Karl, "Imaging of moving targets with multi-static SAR using an overcomplete dictionary," submitted for publication.

[93] C. Cafforio, C. Prati, and F. Rocca, "SAR data focusing using seismic migration techniques," *IEEE Trans. Aerosp. Electron. Syst.*, vol. 27, pp. 194–207, Mar. 1991.

[94] W. Melvin, "A STAP overview," *IEEE Aerosp. Electron. Syst. Mag.*, vol. 19, no. 1, pt. 2, pp. 19–35, 2004.

[95] R. Klemm, *Applications of Space-Time Adaptive Processing*. Edison, NJ: IET, 2004.

[96] G. A. Showman and W. L. Melvin, "Multi-resolution processing to enhance knowledge-aided STAP," in *Proc. 2003 DARPA/AFRL KASSPER Workshop*, 2003.

[97] M. Shahram and P. Milanfar, "On the resolvability of sinusoids with nearby frequencies in the presence of noise," *IEEE Trans. Signal Process.*, vol. 53, pp. 2579–2588, Jul. 2005.

[98] Z.-S. Liu and J. Li, "Implementation of the RELAX algorithm," *IEEE Trans. Aerosp. Electron. Syst.*, vol. 34, pp. 657–664, Apr. 1998.

[99] D. Malioutov, M. Çetin, and A. S. Willsky, "A sparse signal reconstruction perspective for source localization with sensor arrays," *IEEE Trans. Signal Process.*, pp. 3010–3022, Aug. 2005.

[100] S. Cabrera, S. Malladi, R. Mulpuri, and A. Brito, "Adaptive refinement in maximally sparse harmonic signal retrieval," in *Proc. Digital Signal Process. Workshop*, Aug. 2004, pp. 231–235.

[101] L. Scharf and P. Moose, "Information measures and performance bounds for array processors," *IEEE Trans. Inf. Theory*, vol. IT-22, pp. 11–21, Jan. 1976.

[102] M. Shahram and P. Milanfar, "Statistical and information-theoretic analysis of resolution in imaging," *IEEE Trans. Inf. Theory*, vol. 52, pp. 3411–3437, Aug. 2006.

[103] C. D. Austin, R. L. Moses, J. N. Ash, and E. Ertin, "On the relation between sparse reconstruction and parameter estimation with model order selection," *IEEE J. Sel. Topics Signal Process.*, to be published.

[104] R. Baraniuk, V. Cevher, M. Duarte, and C. Hegde, "Model-based compressive sensing," submitted for publication.

[105] Ö. Önhon and M. Çetin, "A nonquadratic regularization-based technique for joint SAR imaging and model error correction," in *Proc. SPIE Algorithms Synthetic Aperture Radar Imagery XVI*, Apr. 2009, vol. 7337, pp. 73370C 1–73370C 10.

[106] P. Schniter, L. Potter, and J. Ziniel, "Fast bayesian matching pursuit," in *Proc. Workshop Inf. Theory Applicat. (ITA)*, La Jolla, CA, Jan. 2008.

[107] M. Elad and I. Yavneh, "A plurality of sparse representations is better than the sparsest one alone," *IEEE Trans. Inf. Theory*, vol. 55, pp. 4701–4714, Oct. 2009.

[108] C. Shannon, "The bandwagon," *IRE Trans. Inf. Theory*, vol. 2, pp. 3–3, Mar. 1956.

ABOUT THE AUTHORS

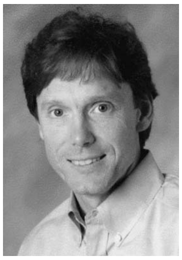

Lee C. Potter (Senior Member, IEEE) received the B.E. degree from Vanderbilt University, Nashville, TN, and the M.S. and Ph.D. degrees from the University of Illinois at Urbana-Champaign, all in electrical engineering. Since 1991, he has been with the Department of Electrical Engineering, The Ohio State University (OSU), Columbus, where he is currently an Associate Professor and investigator at the Davis Heart and Lung Institute. His research interests include statistical signal processing, inverse problems, detection, and estimation, with applications in radar, medical imaging, and networked sensor systems. Dr. Potter is a recipient of the OSU College of Engineering MacQuigg Award for Outstanding Teaching and Lumley Research Award.

Emre Ertin (Member, IEEE) is a Research Assistant Professor with the Department of Electrical and Computer Engineering at the Ohio State University. He received the B.S. degree in Electrical Engineering and Physics from Bogazici University, Turkey in 1992, the M.Sc. degree in Telecommunication and Signal Processing from Imperial College, U.K. in 1993, and the Ph.D. degree in Electrical Engineering from the Ohio State University in 1999. From 1999 to 2002 he was with the Core Technology Group at Battelle Memorial Institute. His current research interests are statistical signal processing, wireless sensor networks, radar signal processing, biomedical sensors, distributed optimization and control.

Jason T. Parker (Member, IEEE) received the B.S. and M.S. degrees in electrical and computer engineering from The Ohio State University, Columbus, in 2004 and 2006, respectively. Since 2006, he has been a research engineer with the Radar Signal Processing branch of the U.S. Air Force Research Laboratory Sensors Directorate. He is concurrently pursuing the Ph.D. in electrical engineering at The Ohio State University. His research interests include compressive sensing, adaptive signal processing, and inverse problems, with applications to radar target detection and imaging.

Müjdat Çetin (Member, IEEE) received the Ph.D. degree in electrical engineering from Boston University, Boston, MA, in 2001. From 2001 to 2005, he was with the Laboratory for Information and Decision Systems, M.I.T., Cambridge, MA. Since September 2005 he has been a faculty member at Sabancı University, Istanbul, Turkey. Dr. Çetin will serve as the Technical Program Co-chair for the International Conference on Pattern Recognition (ICPR) in 2010. He has co-organized the EURASIP Workshop on Sparsity and Compressive Sensing in 2009. He has also served as the Technical Program Co-chair for the IEEE Turkish Conference on Signal Processing, Communications, and their Applications in 2006. He has served in various other organizational capacities, including special session organizer, session chair, and technical program committee member for a number of conferences including the IEEE International Conference on Acoustics, Speech, and Signal Processing; the SPIE Conference on Algorithms for Synthetic Aperture Radar Imagery; the IEEE International Conference on Image Processing; the International Conference on Information Fusion; the IEEE International Symposium on Biomedical Imaging; and the EURASIP European Signal Processing Conference. He is currently an area editor for the Journal of Advances in Information Fusion, and a EURASIP Liaison Officer for Turkey. His research interests include statistical signal and image processing, inverse problems, computer vision, data fusion, wireless sensor networks, biomedical information processing, radar imaging, brain-computer interfaces, machine learning, and sensor array signal processing. Dr. Çetin has received a number of awards including the 2008 Turkish Academy of Sciences Distinguished Young Scientist Award and the 2007 Elsevier Signal Processing Journal Best Paper Award.